

BASIN-SCALE CHANGES IN FLOODPLAIN PALEOSOLS: IMPLICATIONS FOR INTERPRETING ALLUVIAL ARCHITECTURE

MARY J. KRAUS

Department of Geological Sciences, University of Colorado, Boulder, Colorado 80309-0399, U.S.A.
e-mail: Mary.Kraus@colorado.edu

ABSTRACT: Floodplain paleosols in time-equivalent strata of the Willwood Formation differ in terms of paleodrainage and degree of pedogenic development. Ancient soils were more poorly drained and more strongly developed in one area compared to a second area about 45 km away. This difference in drainage is attributed to parent material. The more poorly drained paleosols formed in an area with less permeable, clay-rich floodplain deposits. In the stratigraphic interval that accumulated more slowly, paleosols are more strongly developed, less numerous, and thicker than in the more rapidly accumulating stratigraphic interval. These differences are attributed not only to different sediment accumulation rates, which are commonly considered to control the degree of pedogenic development, but also to differences in avulsion frequency.

A simple model is offered to show how paleosols change with varying basin subsidence rates and the relationship between avulsion frequency and accumulation rate. When avulsion frequency increases more rapidly than sediment accumulation rate, an increase in subsidence rate causes strongly developed paleosols to be overlain by a stratigraphic interval with paleosols that are less well developed, thinner, and more densely spaced. When avulsion frequency is not related to accumulation rate, as early models of alluvial architecture assumed, an increase in subsidence rate produces a stratigraphic section in which strongly developed paleosols are overlain by paleosols that are less well developed, thicker, and more widely spaced. Study of the thickness and degree of development of floodplain paleosols can be used together with more traditional studies of alluvial architecture to provide a clearer understanding of the factors that influenced the stratigraphic architecture in a particular alluvial basin.

INTRODUCTION

Floodplain paleosols vary at several spatial and temporal scales (Kraus and Aslan 1999). Microscale lateral variations in paleosol morphology over distances of tens to hundreds of meters result from short-lived, local processes associated with individual overbank floods. Mesoscale changes, defined by variations over hundreds to thousands of meters away from a channel onto the adjacent floodplain (e.g., catenas and "pedofacies"), reflect autogenic processes such as crevassing and overbank aggradation in local flood basins. Macroscale changes over kilometers to several tens of kilometers reflect larger-scale processes, such as river channel avulsion and broader patterns of floodplain drainage. Basin-scale paleosol variability is generally

controlled by allogenic processes such as regional climate change and tectonic activity.

Spatial variations in paleosols have generally been analyzed at the scale of a channel and its associated floodplain (e.g., Bown and Kraus 1987; Besley and Fielding 1989; Zaleha 1997). Although several studies have examined paleosol variability at larger spatial scales (e.g., Platt and Keller 1992; Joeckel 1995; McCarthy et al. 1997), such studies are difficult without widespread exposures and a means of defining time-equivalent deposits in different locations in the basin. Despite such problems, Kraus and Aslan (1999) suggested that larger spatial scales of paleosol variability potentially could be used to assess autogenic and allogenic factors controlling the distribution of facies and facies architecture in alluvial basins.

This paper is part of a long-term study of diverse floodplain paleosols in the Willwood Formation in the Bighorn Basin of Wyoming. Past work related mesoscale and macroscale paleosol variations to development of fluvial landforms and depositional processes. Bown and Kraus (1987) and Kraus (1987) defined mesoscale pedofacies: lateral changes in paleosols attributed to decreasing accumulation rates away from a channel. Kraus and Aslan (1993) and Kraus (1996) documented macroscale variations defined by vertical alternations between meters-thick avulsion-belt deposits (interbedded sandstones and mudstones with weakly developed paleosols) and finer-grained intervals of overbank deposits with well-developed paleosols.

This paper documents basin-scale paleosol variability in the Willwood Formation. Paleosols are first described and interpreted in terms of ancient soil drainage and degree of development. Paleosols in two parts of the Bighorn Basin with markedly different sediment accumulation rates are compared to examine larger-scale controls on the formation of different kinds of paleosols. Finally, a simple model is presented that relates temporal changes in floodplain paleosols to aggradation rates, avulsion frequency, and alluvial architecture. The model shows how analyzing the thickness and degree of development of floodplain paleosols can contribute to understanding what factors influenced the stratigraphic architecture in a particular alluvial basin.

Geological Setting

The alluvial Willwood Formation was deposited throughout the Bighorn Basin during early Eocene time (Fig. 1). Deposition was associated with structural development of the basin, and sediment was supplied by basin-margin uplifts including the Bighorn and Beartooth ranges (e.g., Neasham and Vondra 1972). Formation of the Absaroka Mountains postdated the deposits described here (Bown 1980).

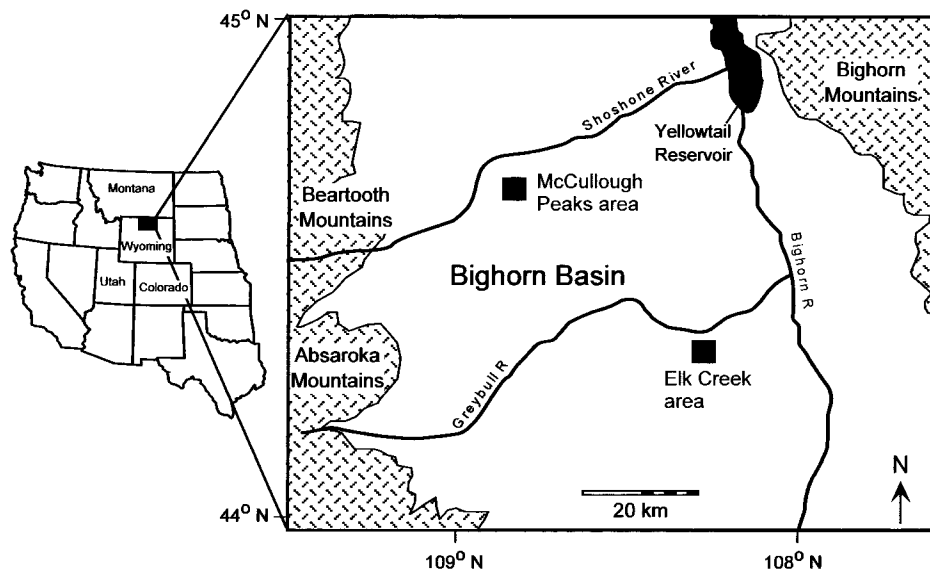


FIG. 1.—Map of the northern half of the Bighorn Basin, Wyoming, showing major mountain ranges surrounding the basin and location of the two study areas in McCullough Peaks and along Elk Creek.

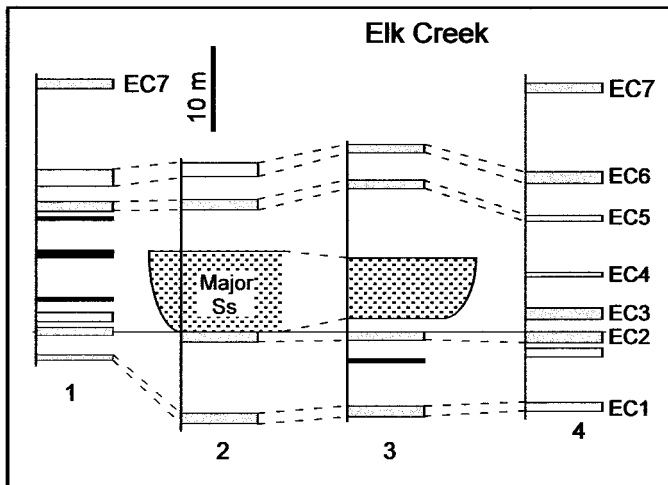
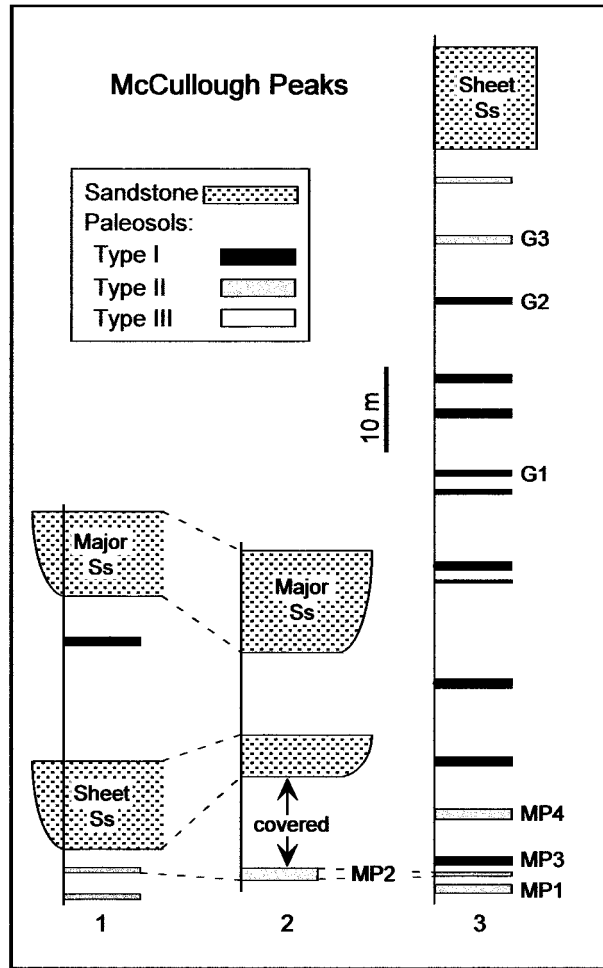
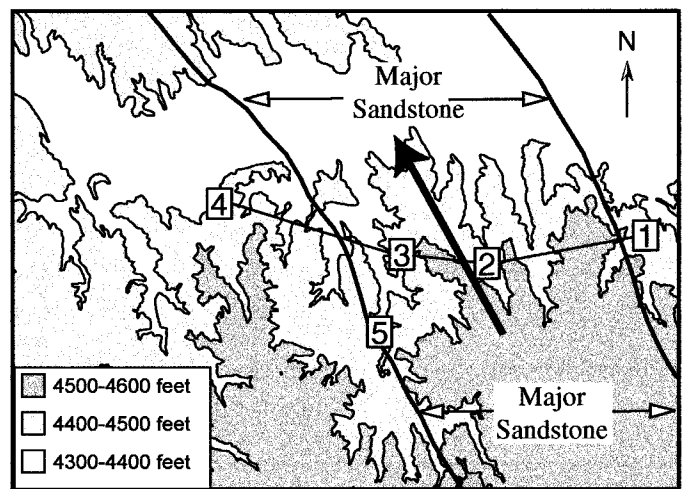
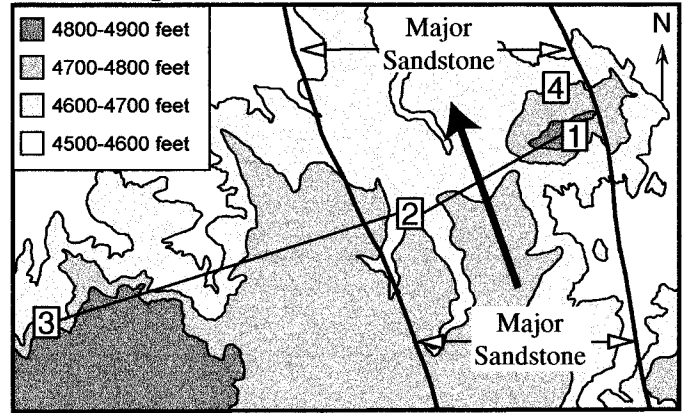


Fig. 2.—Stratigraphic sections in the two study areas showing the stratigraphic levels and thicknesses of the various paleosols and major sandstone bodies. The paleosols shown are the more strongly developed type; they are separated by heterolithic intervals with mudrocks showing weak pedogenesis and small sandstone bodies. Although only some paleosols can be traced laterally in McCullough Peaks, those in Elk Creek can be traced because of excellent exposures. Vertical scale is the same for both cross sections; horizontal scale is schematic. See Fig. 3 and Appendix 1 for locations of stratigraphic sections. MP1 and G1, etc. indicate particular paleosols in McCullough Peaks; EC1, EC2, etc. indicate particular paleosols in Elk Creek section.

McCullough Peaks



Elk Creek

Fig. 3.—Simple topographic maps of the two study areas showing locations of paleosol sections discussed in the text. Heavy lines outline margins of the major sandstone bodies shown in cross sections in Fig. 2. Arrows show summary paleoflow directions. See Appendix 1 for detailed locality information for paleosol sections.

This study examines Willwood paleosols in the McCullough Peaks and Elk Creek areas of the basin (Fig. 1). An interval ~ 70 m thick in McCullough Peaks is compared to an interval ~ 40 m thick in Elk Creek (Fig. 2). Both intervals are well exposed over areas of ~ 10 km² (Fig. 3) and have minimal structural deformation, with dips of 3° or less. A combination of lithostratigraphy, biostratigraphy, and magnetostratigraphy shows that the study intervals are both earliest Eocene in age (Bown et al. 1994; Clyde 1997). Wing et al. (1999) recently revised age estimates for the Willwood Formation in both areas, showing that the two study intervals are approximately coeval. The stratigraphic data also show that strata in the study interval at McCullough Peaks accumulated nearly twice as fast as strata in the Elk Creek interval: 0.56 m/ky versus 0.3 m/ky (Wing et al. 1999).

Willwood plant fossils suggest that mean annual temperature (MAT) reached 18°C during earliest Eocene time (Wing et al. 1999). Following the warm period, MAT dropped to ~ 11°C. The study sections accumulated after this cool period, as the climate warmed again towards a MAT of ~ 18°C. Other paleobotanical studies suggest that precipitation during this time was seasonal (e.g., Wing 1981).

Depositional Setting

The Willwood Formation is a mudrock-dominated fluvial succession that can be subdivided into three major facies (e.g., Kraus and Aslan 1993; Kraus 1996). Thick, laterally extensive sheet sandstones are up to 1.5 km wide and 10 m or more thick (Figs. 2, 3) (Weissmann 1988; Dykstra 1999). These sheet sandstones have been interpreted as the deposits of meandering trunk rivers (e.g., Weissmann 1988; Dykstra 1999). The two other facies, which are each meters thick and which are inter-

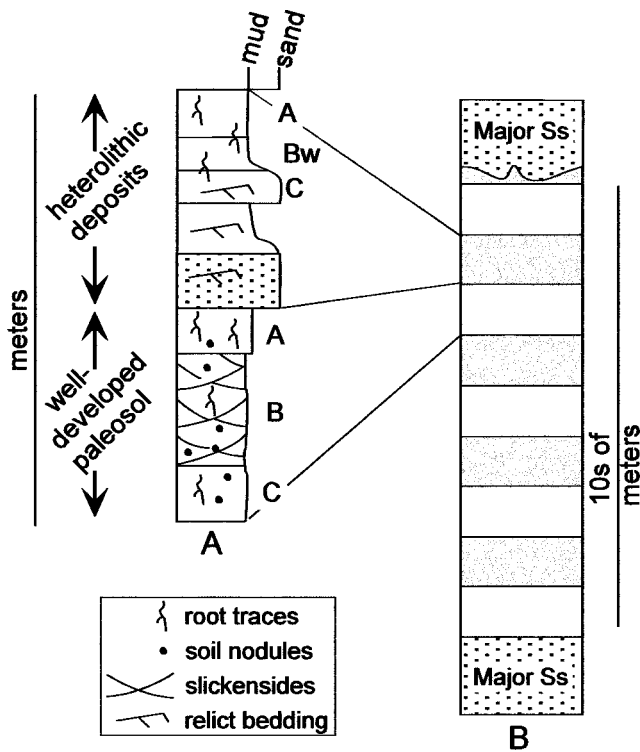


FIG. 4.—Schematic diagram of Willwood floodplain deposits. A) Two kinds of floodplain deposit are recognized on the basis of paleosol properties. Fine-grained deposits with well-developed paleosols are interpreted as overbank deposits. Heterolithic deposits with weakly developed paleosols are interpreted as avulsion deposits. B) At the scale of tens of meters, the two kinds of floodplain deposit are interbedded to form cycles of weak/strong pedogenesis. Major channel sandstones form the top and bottom of the vertical section of floodplain deposits. Those sandstones appear and disappear because of channel avulsion. Letters to the side of column A indicate soil horizons. Bw = weakly differentiated B horizon.

bedded, are (1) heterolithic deposits that consist of ribbon sandstones surrounded by mudrocks with weakly developed paleosols and (2) fine-grained deposits, on which moderately to strongly developed paleosols formed (Fig. 4). Weak pedogenic modification of the heterolithic deposits indicates rapid sedimentation, and those intervals have been interpreted as avulsion deposits that formed on the floodplain by crevasing of the trunk river during avulsion (e.g., Kraus and Aslan 1993; Kraus 1996). The more strongly developed paleosols indicate that the fine-grained parent materials accumulated relatively slowly and episodically, and those materials have been attributed to deposition from overbank flooding of the trunk river. Paleosols that developed on the overbank deposits are the major focus of this study.

METHODS

Morphologic features in the paleosols, including colors, nodule type, and grain size, were described in the field. To standardize field assessment of grain size, representative samples were analyzed quantitatively using laser diffraction with the Malvern Longbed Mastersizer. Each field unit was also described in the laboratory using a binocular microscope. Colors were described from fresh, dry samples.

Clay mineralogy of the < 2 μm fraction of samples was determined using a Scintag X-ray diffractometer with a Cu target. Each sample was analyzed following air-drying, glycolation, and heating to 550°C. Semiquantitative estimates of the abundances of the various clay minerals were made using the computer-determined areas under the (001) peaks of the glycolated samples and the weighting factors of Cook et al. (1975). Major oxide weight percents of representative paleosol samples were determined using X-ray fluorescence of whole-rock samples. Thin sections of representative samples were examined for micromorphologic features.

FLOODPLAIN PALEOSOLS

Quantitative grain-size analyses show that parent material in the McCullough Peaks study section was coarser than that in Elk Creek (Table 1). Particularly dra-

TABLE 1.—Quantitative grain size data for fine-grained Willwood deposits.

Location	Average Clay Content	Percent Claystones	Percent Mudstones	No. of Samples
McCullough Peaks	55%	21%	69%	61
Elk Creek	78%	81%	19%	83

matic is the average clay content of 78% in Elk Creek versus 55% in McCullough Peaks. Mudrocks from the two study areas show similar clay mineralogy. Smectite is the dominant clay mineral (averaging 50% of all samples) and is accompanied by illite (38%) and kaolinite (9%). Individual profiles show no distinct trends, and the different kinds of paleosols show no significant differences in clay mineralogy.

The paleosols are dominated by gray, red, purple, and yellow-brown as both matrix and mottle colors, where matrix color is the dominant color of a bed, and mottles are small areas of a different color (e.g., Sprecher 2001). Gray includes light olive gray (5Y 6/1) and light greenish to greenish gray (5GY 8/1 to 6/1). Most yellow-brown units and mottles are moderate yellow-brown (10YR 5/4) to dark yellowish orange (10YR 6/6). Less commonly yellow-brown refers to light brown (5YR 6/4) to pale brown (5YR 5/2). Red includes hues of 5R and 10R. Most common are dusky red (5R 3/4) and dark reddish brown (10R 3/4), although pale red (5R 6/2) and grayish red (10R 4/2) are present. Purple includes hues of 5P and 5RP with values and chromas of 6/2 to 4/2.

On the basis of color patterns and other pedogenic features, three different kinds of paleosols are recognized in the two study areas.

Type I Paleosols

Morphology and Geochemistry.—Type I paleosols dominate the McCullough Peaks section (Fig. 2). They consist of a gray or yellow-brown mudstone above a red mudstone (Fig. 5). The red mudstone grades downward into a coarser unit that forms the base of the profile. Type I profiles are relatively thin, ranging from 80 to 130 cm thick.

Both gray and red beds contain gray mottles that are irregular in shape to elongate and branching (Fig. 6A). Red rims, commonly < 0.1 mm thick, surround the mottles. Some gray mottles have a purple inner halo and a red outer halo. Yellow-brown mottles, most ranging from several millimeters to 1 cm in diameter, are present in both gray and red beds (Fig. 6B). Some of those in the red beds have red haloes that are more heavily stained than the surrounding matrix. In reflected light, thin sections show small (< 0.1 mm) flecks of red hematite scattered through the yellow-brown mottles but absent from gray mottles. The red particles are densely packed in the red rims of mottles. Small (< 0.8 mm in diameter) yellow-brown nodules are present in some red beds (Fig. 6C). Gray haloes surround yellow-brown nodules as well as some of the yellow-brown mottles (Figs. 6B, 6C). Carbonate nodules (usually < 3 mm in diameter) are found in about half of the red beds examined.

Distinct burrows are typically sparse, but, where present, are characterized by crescentic-shaped, alternating color bands, commonly in red, gray, and yellow-brown (Fig. 6D). Burrow diameters range from 0.2 to 3 mm, and burrow orientations range from horizontal to vertical. Most thin sections show such intense crescentic fabric that individual burrows have been obscured.

Some red beds show slickensides that, in the field, appear as shiny, clay-lined fractures that intersect to form concave-up, dish-shaped structures with amplitudes of ~ 0.5 m and spacings of ~ 1 m. The presence of large slickensides appears to depend partly on grain size, because they are generally lacking in mudstones with less than ~ 60% clay. The slickensides are not related to any tectonic features.

Clay weight percent decreases downwards through the profiles, as does TOC weight percent, except for an increase in the lower part of the red horizon (Fig. 5). Many red profiles show an increase in "clayeyness" (molecular ratio of $\text{Al}_2\text{O}_3/\text{SiO}_2$) in some part of the red horizon. Iron content (measured as Fe_2O_3) increases downward from the gray into the red bed, as does the Fe/clay ratio, indicating some downward movement of both clay and iron.

Base loss, or the ratio of alumina to bases (CaO, MgO, K_2O , and Na_2O) is one measure of the intensity of weathering because it reflects hydrolysis (e.g., Retallack 1990; Mora and Driese 1999). As weathering increases, bases are depleted, and the ratio increases. Values of base loss for the representative Type I profile increase downwards from the overlying avulsion deposits. They reach a maximum value of ~ 1.5 about 40 cm from the top of the profile, before declining. The unusual rise in base loss towards the bottom of the profile corresponds to a drop in clay content and probably reflects parent material rather than weathering.

Interpretation.—The gray bed is interpreted as an A horizon on the basis of its higher TOC and lower iron content compared to the underlying red bed, which is interpreted as the B horizon. The red color indicates that the B horizon was at least moderately well drained and oxidizing (e.g., Kaempff and Schwertmann 1982;

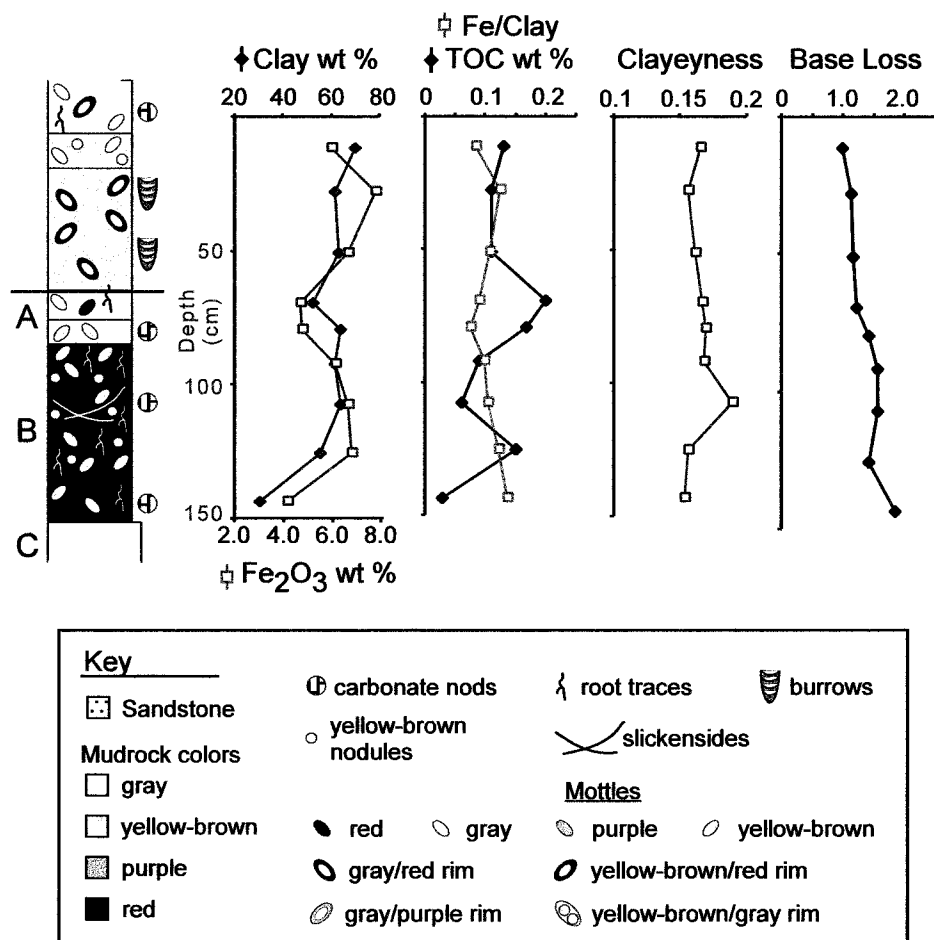


Fig. 5.—Morphologic, textural, and chemical data for a representative type I paleosol profile. A = A horizon; B = B horizon; C = C horizon. Above the paleosol profile are fine-grained deposits showing weak pedogenic development and interpreted as avulsion deposits. Paleosol G2 at location 3 in McCullough Peaks. See Fig. 2 for stratigraphic position of G2 and Fig. 3 and Appendix 1 for location of section.

Schwertmann 1993); however, the mottles, nodules, and slickensides indicate that type I soils underwent seasonal wetting and drying. The mottles and yellow-brown nodules are redoximorphic features, which resulted from changes in the redox conditions of the soil in response to fluctuations in soil saturation (e.g., Vepraskas et al. 1992; Vepraskas 1994). Gray mottles and haloes are a kind of iron depletion, which formed when the soil was saturated and iron was reduced and removed from an area (e.g., Duchaufour 1982; Fanning and Fanning 1989). Many were probably root channels or burrows, which are especially prone to the reduction and removal of iron oxides because organic material was present (e.g., Schwertmann 1993). Reduced iron and manganese can be leached from the soil or precipitated in more oxidized areas of the soil as mottles and/or nodules. The red rims around gray and yellow-brown mottles and the yellow-brown nodules represent iron concentrations, formed by the reprecipitation of iron in better-oxidized areas. The burrows are attributed to earthworms, which, in modern soils, commonly leave vermiforms like those seen in the thin sections (FitzPatrick 1993).

The gray color of the A horizon or the yellow-brown A horizon found in other Type I paleosols probably reflects reducing conditions related to seasonal wetness and to the higher organic content in the upper part of the profile (e.g., Macedo and Bryant 1987, 1989). Red soils in the tropics and subtropics commonly have a yellow A horizon above a red B horizon (e.g., Kaempff and Schwertmann 1982), and the yellow-brown colors are characteristic of red soils with intermediate drainage (Macedo and Bryant 1987). Macedo and Bryant (1987, 1989) attributed this phenomenon to the selective dissolution of hematite caused by weak reduction related to seasonal wetness and the high organic content and roots in the upper part of the profile. Similarly, the yellow-brown mottles in the B horizon, especially those with heavy red rims, suggest that hematite was preferentially removed from some areas of the B horizon, leaving behind only goethite. Local removal of hematite, but not goethite, indicates weakly reducing conditions, suggesting that periods of seasonal wetting were short (e.g., Stolt et al. 1994).

Following Duchaufour's (1982) classification, the type I paleosols are Fersiallitic soils, which are usually characterized by yellow-brown A horizons and red B horizons due to rubification (reddening due to hematite formation). Fersiallitic soils,

which have no direct equivalent in the Soil Survey (1975, 1998) classification, are characterized by 2:1 clays (smectites) and slickensides, especially if smectite is abundant. Although most of the type I paleosols differ from Fersiallitic soils in that no Bt horizon formed and iron and clay did not typically co-migrate, those processes may have been inhibited by the relatively high clay content of the Willwood paleosols. Fersiallitic soils commonly form in climates with MAT between 13 and 20°C and seasonally spaced rainfall (Duchaufour 1982), conditions that characterized the Bighorn Basin when the paleosols formed. The relatively thin soil profiles, and base-loss values that are only somewhat higher than for the overlying avulsion deposits, are consistent with fersiallitic weathering, which is comparatively weak.

Type II Paleosols

Morphology and Geochemistry.—Type II paleosols are present in both study areas but dominate the Elk Creek section. Profiles range between 150 and 200 cm thick and commonly consist of a yellow-brown or gray bed underlain by a purple-red couplet or a red-purple-red sequence (Fig. 7). About half of the red and purple beds with clay content > 60% show slickensides that define pseudoanticlinal structures ranging from 0.5 m to nearly 1 m in height and from 2 to 3 m in spacing. Type II paleosols can change laterally to a type III paleosol, which lacks a red bed (Fig. 2).

The yellow-brown bed contains gray mottles with red rims. Underlying red units have yellow-brown mottles and nodules, and gray mottles with haloes of a deeper red than the matrix are common. Red units regularly contain small carbonate nodules, and thin sections show the presence of micro-accumulations of calcite (Fig. 8). Some micro-accumulations are nodular and range from ovoid to irregular in shape with long axes less than ~ 0.5 mm long. Other accumulations are elongate with a long dimension < 1 mm. Most consist of micrite or microspar with crystal sizes of ~ 0.05 mm, although some examples have coarser spar in the center of the accumulation. Most are present within gray mottles, but some are present in the red matrix.

Thin sections show that purple matrix is characterized by widely dispersed red

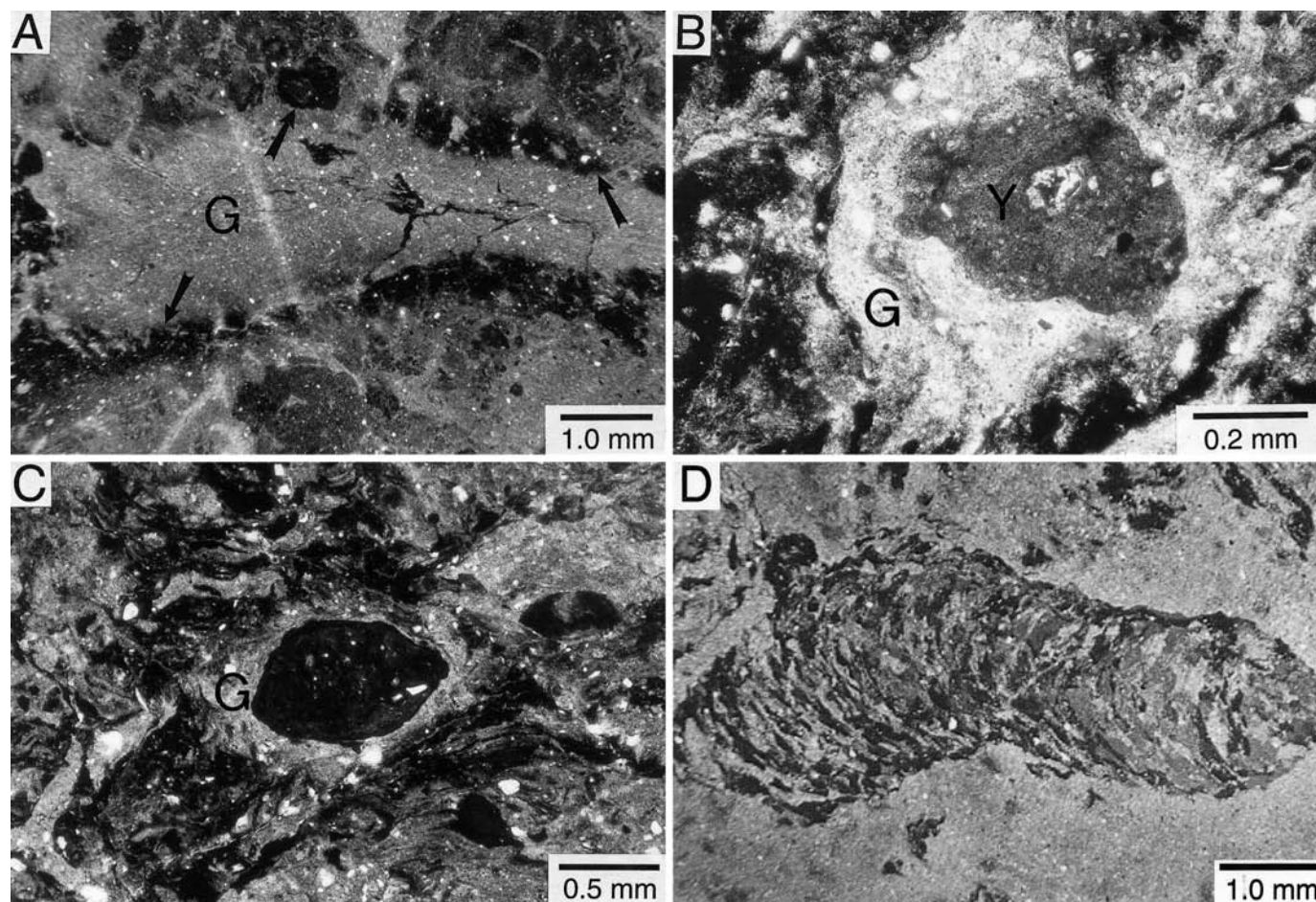


FIG. 6.—Photomicrographs of paleosol features. **A**) Elongate gray mottle (G) with red rim shown by arrows. Dark strands in the center of the mottle may be remnants of a root. Plane-polarized light. **B**) Yellow-brown mottle (Y) surrounded by gray halo (G). Plane-polarized light. **C**) Yellow-brown nodule surrounded by a gray halo (G). Plane-polarized light. **D**) Burrow with crescentic, alternating color bands in red, yellow-brown, and gray. Plane-polarized light.

microspheres ($< 5 \mu\text{m}$ in diameter), whose color indicates that they consist of hematite, and the absence of any yellow-brown stain except as distinct mottles or nodules. Purple units contain both yellow-brown and gray mottles. The gray mottles are depleted in Fe_2O_3 and MnO relative to the purple matrix, and the yellow-brown mottles are enriched in Fe_2O_3 and MnO relative to the purple matrix (Kraus and Aslan 1993). Many yellow-brown mottles and nodules are present as small clusters of several mottles and/or nodules that are separated from one another, and from the surrounding purple matrix, by gray depletion zones. Some purple beds have yellow-brown mottles with red rims, and thin sections show that some purple beds contain scattered, crescent-shaped red mottles whose shape indicates they were once part of burrows (Fig. 9). In addition, some purple beds contain microscopic carbonate nodules or irregular accumulations of micrite in gray mottles.

An unweathered exposure beneath a sandstone ledge provides an unusual opportunity to examine the relationship between purple and red paleosol units (Fig. 10). A prominent feature of the upper red bed in this example is that it contains large, downward-branching soil channels that are dominantly purple, although with gray centers. The purple-colored soil channels progressively enlarge and merge downward to form the underlying purple unit. Laterally, the purple bed shows an increase in red mottles and, over the ~ 10 m of the exposure, it changes to a red bed with large purple soil channels.

Most, although not all, gray or yellow-brown beds at the tops of profiles show higher TOC contents than lower parts of the profiles (Fig. 7). Clay weight percent decreases downward through profiles; however, the measure of clayeyness shows little if any downward trends. Iron content (measured as Fe_2O_3) usually shows weak downward increases, as do Fe/clay ratios, suggesting only weak downward movement of iron. Most type II paleosols show initial down-profile increases in base loss. Maximum base-loss ratios reach higher values than for type I paleosols, usually between 1.75 and 2.0, and higher values (> 1.5) are maintained to a greater depth than in type I paleosols.

Interpretation.—The down-profile geochemical trends and the color patterns in the paleosols indicate that much of the iron movement in the profiles was intrahorizontal rather than interhorizontal. No Bt horizons can be recognized; down-profile clay movement was probably inhibited by the high clay content, and thus low permeability, of the parent material (e.g., Duchaufour 1982).

The red part of the B horizon indicates that rubification was an important soil process. Various features suggest that purple beds originally had more abundant hematite and that they were partly leached of hematite because of iron reduction and removal, but not to the degree that gray beds were bleached. First, thin sections show that red microspheres are widely dispersed in purple matrix and mottles, densely packed in red matrix and mottles, and absent in gray areas, suggesting that those three colors are the result of variations in hematite concentrations. Second, within a purple bed, the purple matrix has higher values of Fe_2O_3 than gray zones, but lower values of Fe_2O_3 than yellow-brown mottles. Third, expansion of purple soil channels downward into a red bed suggests that beds became purple over time as a result of bleaching along soil channels (Fig. 10). Finally, red mottles are present in the purple matrix but only as small relicts that show signs of leaching (Fig. 9).

Several features indicate that purple colors resulted from surface-water gleization. First, the purple color is associated with iron reduction and mobilization that took place along soil channels, which is characteristic of surface-water gley (e.g., Fanning and Fanning 1989). Second, in the field example described above, the purple soil channels descend from a higher unit, also suggesting surface-water gley (e.g., Wright et al. 2000).

The various paleosol horizons can be assigned to different surface-water gley stages established by PiPujol and Buurman (1994). Early gley stages show incipient development of gray mottles or bleached zones and faint iron-rich rims around those. As gleizing continues, the bleached zones enlarge and the red rims intensify. Eventually, by stage 5, the depletion channels have expanded to the point that the iron-rich rims show significant dissolution, as seen in the purple beds of stage II paleo-

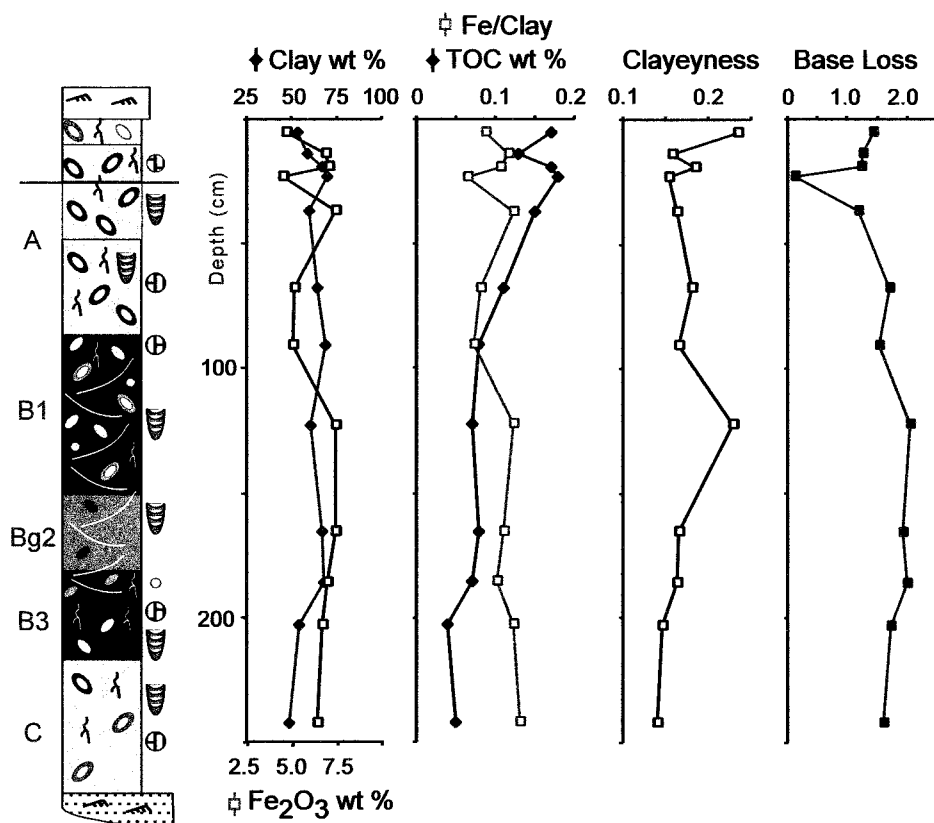


FIG. 7.—Morphologic, textural, and chemical data for a representative type II paleosol profile. MP1 from location 4 in McCullough Peaks. Bg = gleyed B horizon; B1, B2, etc. indicate subdivisions of the B horizon based on different morphologic attributes. See Fig. 5 for key to symbols, Fig. 2 for stratigraphic position of MP1, and Fig. 3 and Appendix 1 for section location.

sols. Consequently, the upper, purple part of the B horizon shows strong surface-water gleying, and it is designated as a Bg (gleyed B) horizon. The intensity of gleying decreases in the lower part of the B horizon.

The high clay content of the paleosols, the dominance of smectite in the clay fraction, and the presence of well-developed slickensides indicate that the paleosols are vertic paleosols (e.g., Soil Survey Staff 1975, 1998; Duchaufour 1982). Modern Vertisols form where parent materials are rich in 2:1 clays, as a result of deposition or authigenesis. Alternating episodes of soil wetting and drying produced the slickensides (e.g., Yaalon and Kalmar 1978; Wilding and Tessier 1988). Although marked dry and rainy seasons are needed for the shrink-swell processes, Vertisols develop under a wide range of moisture conditions. The redoximorphic features that are so prominent in type II paleosols are characteristic of Aquerts, which may be dry for only a few weeks each year (e.g., Buol et al. 1997). At the same time, the

dry season was sufficient to produce microscopic calcite accumulations in some purple beds. The microscopic accumulations resemble the type C6 calcite accumulation of PiPujol and Buurman (1997), which they attributed to formation in seasonal climates during the dry season. Episodic rains introduce water into the soil channels, and, if the water contains calcium carbonate, micrite precipitates when the soil dries.

The high clay content of Vertisols can itself contribute to the poor drainage of these soils. In addition, water infiltration depends not only on the length of the wet season but also on how rainfall is spaced (e.g., Wilding and Tessier 1988; Wambeke 1992). If the rainy season begins with heavy rains, water can descend through soil channels and reach the lower part of the profile. In contrast, if the early rains are light, the upper part of the solum may become saturated such that soil swelling

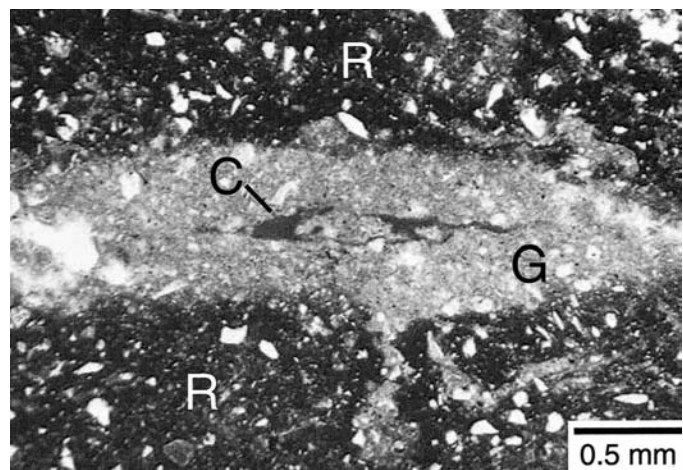


FIG. 8.—Gray depletion channel (G) with thick red rim (R). Small, micrite accumulation (C) is present in the center of the depletion. Plane-polarized light.

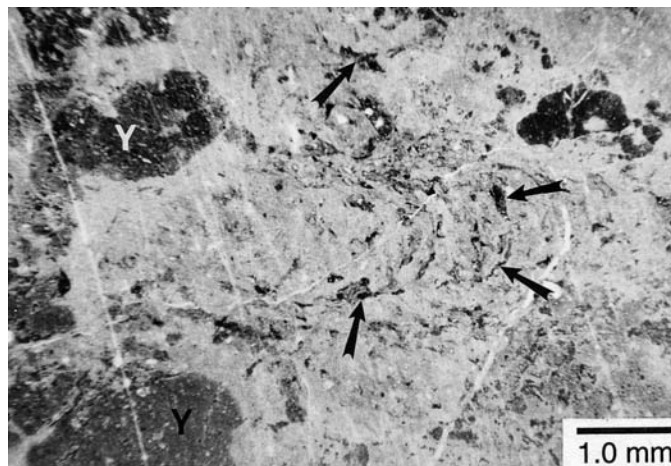


FIG. 9.—Photomicrograph of a purple mudrock showing relict red mottles (arrows). The crescentic shape indicates that the red, hematitic areas are remnants of a burrow. Yellow-brown mottles (Y) also present in purple matrix. Plane-polarized light plus reflected light.

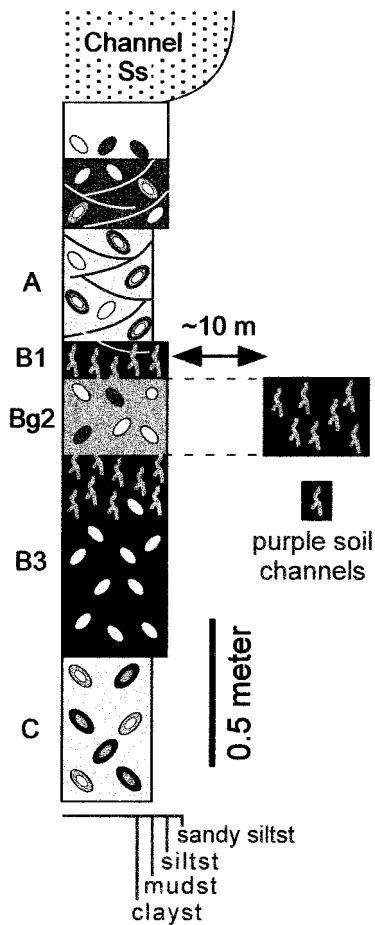


FIG. 10.—Lateral change from a purple bed (Bg2 horizon) to a red bed over a distance of ~ 10 m. Purple soil channels descending from overlying B1 horizon have expanded and merged to create the purple bed. Type II paleosol (EC3) from Elk Creek at location 5. Bg = gleyed B horizon; B1, B2, etc. indicate subdivisions of the B horizon based on different morphologic properties. See Fig. 5 for key to symbols, Fig. 2 for stratigraphic position of EC3, and Fig. 3 and Appendix 1 for location of section. See text for details.

closes the soil channels. In that case, the lower part of the solum may remain dry and surface-water gley conditions can be established.

The strong surface-water gleying represented by the Bg horizon indicates that stage II paleosols were more poorly drained than stage I paleosols. The base-loss trends and values indicate that type II paleosols were also more strongly weathered than type I paleosols and, together with the thicker paleosol profiles, suggest that the type II paleosols represent a longer period of pedogenic development than type I paleosols.

Type III Paleosols

Morphology and Geochemistry.—In Elk Creek, Type II paleosols locally change to type III paleosols. In addition, two paleosols in Elk Creek (EC4 and EC6 in Fig. 2) are type III paleosols over most of their exposed lateral extent but change locally to a type II paleosol. A type III paleosol profile consists of a gray bed above a purple bed or a yellow-brown and purple sequence (Fig. 11). Profiles range from ~ 150 cm to nearly 300 cm thick.

Gray beds at the top of the profile contain red-rimmed, gray mottles and yellow-brown mottles. The purple beds resemble those in the type II paleosols in the presence of abundant yellow-brown mottles and nodules. Large slickensides similar to those in type II paleosols are also present in the clay-rich purple beds; however, neither carbonate accumulations nor relict red mottles are found. In most examples, the purple bed of a type III profile grades downward into yellow-brown units containing gray root mottles with red haloes or compound haloes with an inner purple and outer red zone. Locally, paleosol EC6 is a compound paleosol with two type III profiles (Fig. 11).

Profiles commonly show a TOC maximum in the uppermost gray bed, and TOC decreases downward into the purple unit and remains low (Fig. 11). Clay weight percent decreases downward through profiles, and a measure of clayeyness shows little if any trend in most profiles. In most examples, the upper gray bed is depleted in iron (measured as Fe_2O_3) compared to purple and yellow-brown units below, which are relatively enriched. Most profiles show no correspondence between down-profile iron and clay trends. Base-loss values are high (values of ~ 2.0) compared to the other kinds of paleosols, and they remain high to a considerable depth.

Interpretation.—Like type II paleosols, type III paleosols are interpreted as vertic paleosols on the basis of their high clay content, dominance of 2:1 clays, and local presence of well-developed slickensides. Type III paleosols lack the lower red B horizon characteristic of type II paleosols, suggesting that the entire B horizon was strongly gleyed. In addition, the absence of relict red mottles and calcite microaccumulations, which are present in the purple Bg horizon of many type II paleosols, suggests that conditions were too wet to form calcite or to preserve any red areas. Thus, the entire B horizon underwent intense surface-water gleying, and type III paleosols represent more poorly drained conditions than either type I or type II paleosols. Lateral changes between type II and type III paleosols are attributed to local changes in drainage on the ancient floodplain (Figs. 3, 10).

The unusually thick and laterally persistent type III paleosol towards the top of the study interval (EC6) is attributed to a lengthy episode of paleosol development compared to other paleosols at either study location. The high base-loss values and depths to which those values extend are consistent with more prolonged pedogenesis. This paleosol may have formed on a more distal part of the floodplain, where its lower topographic position resulted in a hydromorphic paleosol and slower sediment accumulation rates produced a more strongly developed paleosol than the type II paleosols in this section.

CONTROLS ON PALEOSOL VARIATIONS

McCullough Peaks is dominated by type I paleosols; type II paleosols are present, and type III paleosols are absent (Fig. 2). Although type II paleosols dominate the Elk Creek study section, type III paleosols are present as are sparse type I paleosols. Differences between the two areas are attributed to differences in drainage and degree of soil development.

Drainage Variations

Judging from paleocurrent data showing northwest drainage during early Eocene time (Fig. 1), the better-drained paleosols in McCullough Peaks were down paleoslope from the more poorly drained paleosols that characterize Elk Creek. This suggests that down-basin slopes did not control basin-scale paleosol variations. The floodplain deposits in Elk Creek are finer grained than those in McCullough Peaks (Table 1), implying that the variations in drainage are linked to variations in grain size and, thus, in permeability. The surface-water gley features that are so characteristic of the Elk Creek paleosols are consistent with the clay-rich parent material and the development of perched water tables. The paleosols in McCullough Peaks contain less clay, and this is reflected in the absence of significant surface-water gley attributes.

Degree of Soil Development

The presence of more strongly developed paleosols in the Elk Creek area is consistent with slower rates of sediment accumulation there compared to McCullough Peaks (e.g., Kraus and Bown 1986; Wright 1992). The different degree of soil development is also attributed to different frequencies of channel avulsion in the two areas. Because an avulsion deposit is several meters thick and was deposited rapidly (on the order of 10^2 years), its deposition terminated formation of the paleosol below (Fig. 4). Thus, the time available for paleosol development was the time between successive avulsion deposits. Judging from the sediment accumulation rates of 0.56 m/ky for the section in McCullough Peaks and 0.3 m/ky for the section in Elk Creek (Wing et al. 1999), section 3 in McCullough Peaks (70 m) and section 4 in Elk Creek (38 m) represent approximately equal amounts of time. Both sections consist of a series of paleosols with no major channel sandstones, and both are a similar distance from laterally equivalent major sandstone bodies. The McCullough Peaks section has more paleosols (12) than does the equivalent section in Elk Creek (9 paleosols), each of which is separated by avulsion deposits. Consequently, for the time represented by the two stratigraphic sections, avulsion deposits were more frequent in McCullough Peaks, and paleosols there are less strongly developed.

Because avulsion deposits are spatially limited, individual deposits did not cover the entire floodplain, and the time between avulsion deposits is not identical to avulsion frequency. Nonetheless, the number of avulsion deposits through a stratigraphic interval should depend on avulsion frequency, and paleosol development should be related to avulsion frequency.

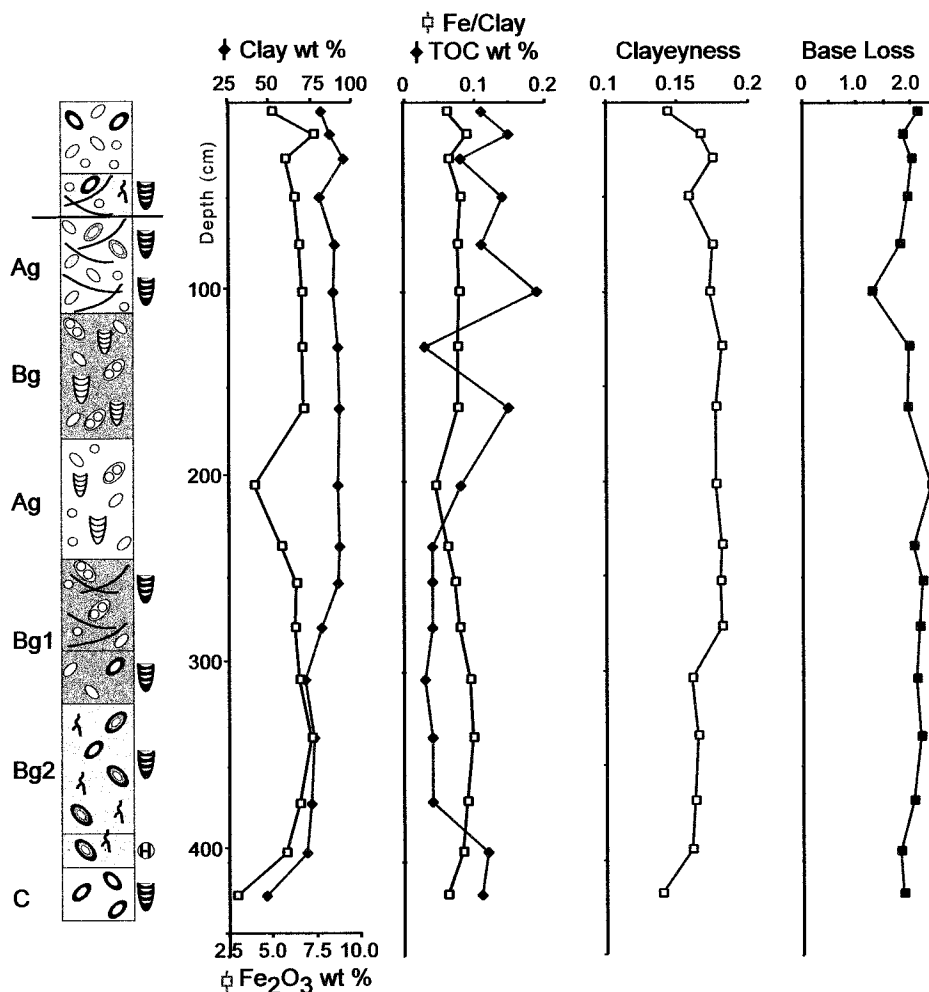


FIG. 11.—Morphologic, textural, and chemical data for two representative type III paleosols, which, in this example, are vertically stacked profiles. Above the strongly developed profiles are fine-grained deposits showing weak pedogenic development and interpreted as avulsion deposits. The paleosols represent EC6 at location 2 in Elk Creek. Ag and Bg = gleyed A and B horizons; B1 and B2 indicate subdivisions of the B horizon based on different morphologic properties. See Fig. 5 for key to symbols, Fig. 2 for stratigraphic position of EC6 and Fig. 3 and Appendix 1 for location of section.

ALLUVIAL ARCHITECTURE

The relationship between degree of paleosol development and frequency of avulsion seen in the two study areas has implications for models of alluvial architecture (AA models), which examine the primary controls on the proportion and stacking patterns of channel sandstones in avulsion-dominated fluvial systems. In those models, the floodplain deposits are merely background for the channel sandstones; no lithologic or pedologic details are provided. In light of the Willwood paleosols, a simple model is offered here to show how paleosols change with varying basin subsidence rates and how the paleosols can help decipher the architecture of individual alluvial successions.

Early AA models showed that subsidence rates are a major control on the degree to which channel sandstones are connected (Allen 1978; Leeder 1978; Bridge and Leeder 1979). When subsidence rates (sediment accumulation rates) are low, sandstone bodies show numerous interconnections and the ratio of fine-grained deposits to sandstone is low (Fig. 12A). As subsidence rates increase, connections between sandstone bodies diminish and the ratio of fine-grained deposits to sandstone increases.

Those early models assumed that avulsion frequency remained constant as subsidence rate (accumulation rate) changed; however, later models related avulsion frequency to accumulation rate. Avulsion was assumed to occur when the channel belt aggraded to a critical height above the floodplain (e.g., Bryant et al. 1995; Heller and Paola 1996; Mohrig et al. 2000). This critical relief developed by differential sedimentation in the channel belt relative to that on the floodplain; thus, higher aggradation rates cause avulsion frequency to increase. Bryant et al. (1995) proposed that avulsion frequency is proportional to r^b , where r is accumulation rate and b is an exponent that can vary from 0 to greater than 1. Those authors and Heller and Paola (1996) demonstrated that the alluvial architecture, as expressed in the thickness and connectivity of channel sandstone bodies, depends on the relation between avulsion frequency and sediment accumulation rate. If avulsion frequency changes

linearly with the rate of sediment accumulation ($b = 1$), the sandstone bodies show no change in connectivity or spacing in response to an increase in accumulation rate over time (Fig. 12B). The ratio of fine-grained deposits to sandstone also remains unchanged. If avulsion frequency increases more quickly than accumulation rate ($b > 1$), an increase in sedimentation rate produces greater connectivity among sandstone bodies and a decrease in the ratio of fine-grained deposits to sandstone (Fig. 12C).

A simple model is proposed that relates paleosol maturity and abundance to changes in basin subsidence for the three different relationships between avulsion frequency and accumulation described above (Fig. 13). The model mirrors those of Bryant et al. (1995) and Heller and Paola (1996); however, the fine-grained deposits, rather than the sandstone bodies, are emphasized. The model considers a fluvial section where accumulation rates increased twofold (the upper two-thirds of the section is two times thicker than the lower third). Paleosols change predictably upward through the section depending on how avulsion frequency changed in response to the up-section change in accumulation rate.

For the simplest case, $b = 1$, avulsion frequency increases linearly with accumulation rate (Fig. 13A). Because the upper part of the section is twice as thick as the lower part of the section, twice as many avulsions took place as it was deposited. Twice as many paleosols are present in the upper section (6 vs. 3); however, those paleosols are more weakly developed than those in the lower part of the section. At low values of b ($b \ll 1$), avulsion frequency is effectively constant, and the lower and upper parts of the cross section have an equal number of paleosols (Fig. 13B). Paleosols in the upper, more rapidly deposited part of the section are thicker and more weakly developed because the rapid accumulation rates resulted in the deposition of more fine-grained sediment between avulsions. If avulsion frequency increases more rapidly than sediment accumulation rate increases ($b > 1$), the number of paleosols in the upper part of the section is more than twice the number present lower in the section (7 vs. 3; Fig. 13C). Those paleosols are thinner because, with more frequent avulsion, less fine-grained sediment is deposited on the floodplain

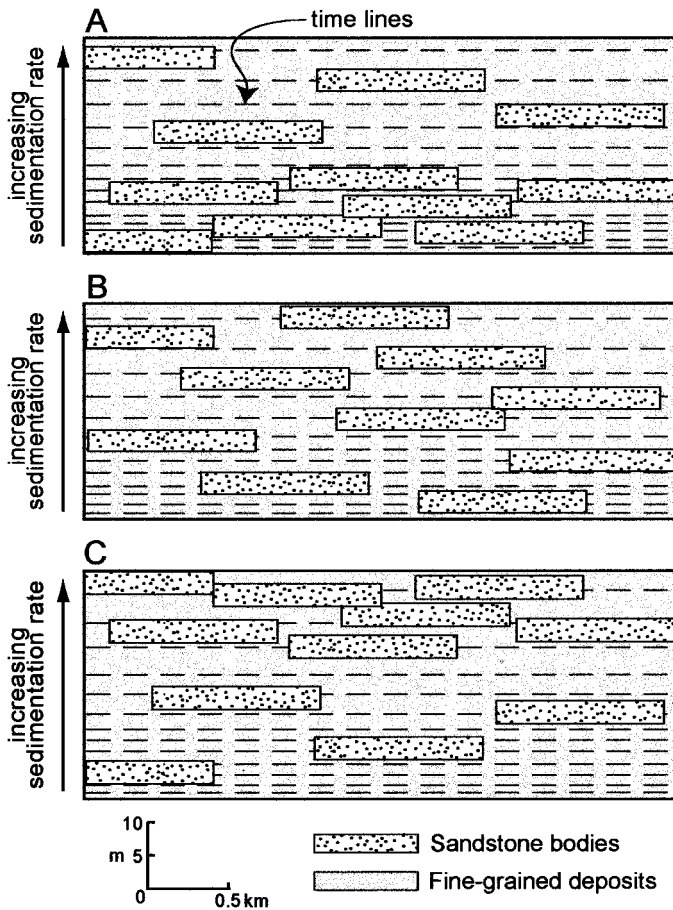


FIG. 12.—Models of alluvial architecture that predict how interconnectedness of sandstone bodies changes as sediment accumulation rate increases and for different relationships between avulsion frequency and accumulation rate. A) Early models assumed that avulsion frequency did not change as accumulation rate increased (i.e., $b \ll 1$). B) Avulsion frequency changes linearly with accumulation rate ($b = 1$). C) Avulsion frequency increases more rapidly than accumulation rate ($b > 1$). See text for details. Modified from Heller and Paola (1996).

between successive avulsion deposits. The cross section suggests that paleosol spacing also becomes denser as accumulation rate increases.

Paleosol models can help constrain parameters in AA models. Careful analysis of the paleosols in different parts of the stratigraphic column should provide clues as to the local relationship between avulsion frequency and sediment accumulation rates (i.e., the value of b). Study of the thickness and degree of development of the paleosols together with analysis of the thickness and multistory character of the sandstone bodies should provide a clearer understanding of what factors influenced the stratigraphic architecture in a particular alluvial basin.

CONCLUSIONS

Two time-equivalent stratigraphic intervals in the Willwood Formation contain floodplain paleosols that differ in terms of drainage and degree of development. Drainage variations over tens of kilometers are commonly attributed to topographic or climatic variations. Willwood vertic paleosols, which were poorly drained, formed in the study area where floodplain sediments were clay rich.

The two study areas had strongly contrasting subsidence rates. More numerous, thinner, and more weakly developed Fersiallitic paleosols dominate the more rapidly subsiding study area. These differences are attributed to more rapid sediment accumulation rates and more frequent avulsion in the rapidly subsiding study area.

A simple paleosol architecture model shows how floodplain paleosols vary in response to changes in basin subsidence and to variations in the relation between avulsion frequency and sediment accumulation rates.

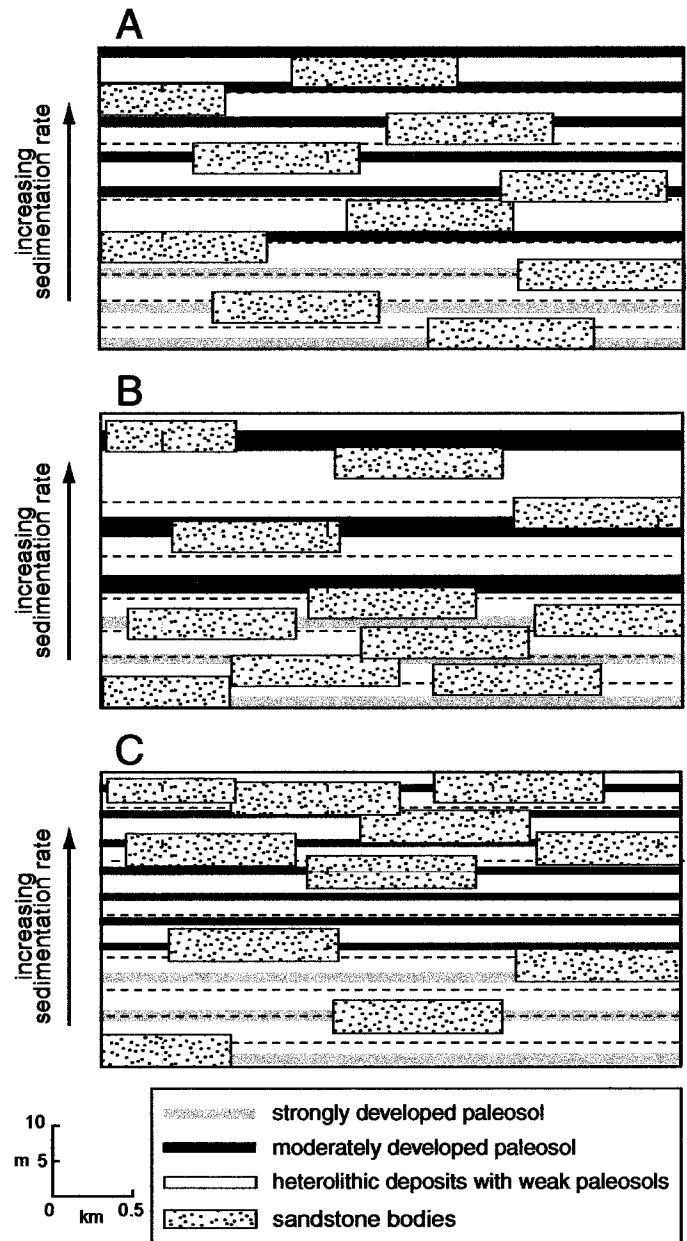


FIG. 13.—Three models that predict paleosol thickness, degree of development, spacing, and numbers for different relationships between avulsion frequency and accumulation rate (i.e., for different values of b). The upper part of each section had an accumulation (subsidence) rate that was two times as fast as in the lower part of each section. A) Avulsion frequency changes linearly with accumulation rate ($b = 1$). B) Avulsion frequency is effectively constant as sediment accumulation rate increases; $b \ll 1$. C) Avulsion frequency changes more rapidly than accumulation rate ($b > 1$). Dashed lines represent time lines. See text for details. Sandstone part of diagrams modified from Heller and Paola (1996).

ACKNOWLEDGMENTS

This research was supported by National Science Foundation Grant EAR-9706115 to MJK. I thank A. Pulham for informative discussion of the sandstone bodies and alluvial architecture models. The manuscript has benefited from constructive reviews by Brian Willis, Paul Wright, and associate editor Steve Driese. Appendix 1 is found in the SEPM data archive at <http://www.ngdc.noaa.gov/mgg/sepm/archive/index.html>.

REFERENCES

- ALLEN, J.R.L., 1978, Studies in fluvial sedimentation: an exploratory quantitative model for the architecture of avulsion-controlled alluvial suites: *Sedimentary Geology*, v. 21, p. 129–147.
- BESLY, B.M., AND FIELDING, C.R., 1989, Palaeosols in Westphalian coal-bearing and red-bed sequences, central and northern England: *Palaeogeography, Palaeoclimatology, Palaeoecology*, v. 70, p. 303–330.
- BOWN, T.M., 1980, Summary of latest Cretaceous and Cenozoic sedimentary, tectonic, and erosional events, Bighorn Basin, Wyoming, in Gingerich, P.D., ed., *Early Cenozoic Paleontology and Stratigraphy of the Bighorn Basin, Wyoming*: University of Michigan, Papers on Paleontology, no. 24, p. 5–32.
- BOWN, T.M., AND KRAUS, M.J., 1987, Integration of channel and floodplain suites in aggrading fluvial systems. I. Developmental sequence and lateral relations of lower Eocene alluvial paleosols, Willwood Formation, Bighorn Basin, Wyoming: *Journal of Sedimentary Petrology*, v. 57, p. 587–601.
- BOWN, T.M., ROSE, K.D., SIMONS, E.L., AND WING, S.L., 1994, Distribution and stratigraphic correlation of fossil mammal and plant localities of the Fort Union, Willwood, and Tatman Formations (upper Paleocene–lower Eocene), central and southern Bighorn Basin, Wyoming: U.S. Geological Survey, Professional Paper 1540.
- BRIDGE, J.S., AND LEEDER, M.R., 1979, A simulation model of alluvial stratigraphy: *Sedimentology*, v. 26, p. 617–644.
- BRYANT, M., FALK, P., AND PAOLA, C., 1995, Experimental study of avulsion frequency and rate of deposition: *Geology*, v. 23, p. 365–368.
- BUOL, S.W., HOLE, F.D., McCracken, R.J., AND SOUTHARD, R.J., 1997, *Soil Genesis and Classification*, 4th Edition: Ames Iowa, Iowa State University Press, 527 p.
- CLYDE, W.C., 1997, Stratigraphy and mammalian paleontology of the McCullough Peaks, northern Bighorn Basin, Wyoming: implications for biochronology, basin development, and community reorganization across the Paleocene–Eocene boundary [unpublished Ph.D. thesis]: University of Michigan, Ann Arbor, 271 p.
- COOK, H.E., JOHNSON, P.D., MATTI, J.C., AND ZEMMELS, T., 1975, Methods of sample preparation, and X-ray diffraction data analysis, in Kaneps, A.G., ed., *Initial Reports of the Deep Sea Drilling Project*: Washington, D.C., U.S. Government Printing Office, v. 28, p. 999–1007.
- DUCHAUFOUR, P., 1982, *Pedology*: London, Allen & Unwin, 448 p.
- DYKSTRA, M., 1999, Fluvial architecture in the lower Eocene Willwood Formation, northwestern Wyoming as an indicator of avulsion style [unpublished M.S. thesis]: University of Colorado, Boulder, 59 p.
- FANNING, D.S., AND FANNING, M.C.B., 1989, *Soil: Morphology, Genesis, and Classification*: New York, Wiley & Sons, 395 p.
- FITZPATRICK, E.A., 1993, *Soil Microscopy and Micromorphology*: Chichester, U.K., Wiley & Sons Ltd, 304 p.
- HELLER, P.L., AND PAOLA, C., 1996, Downstream changes in alluvial architecture: an exploration of controls on channel-stacking patterns: *Journal of Sedimentary Research*, v. 66, p. 297–306.
- JOECKEL, R.M., 1995, Paleosols below the Ames Marine Unit (Upper Pennsylvanian, Cone-maugh Group) in the Appalachian Basin, U.S.A.: variability on an ancient depositional landscape: *Journal of Sedimentary Research*, v. A65, p. 393–407.
- KAEMPF, N., AND SCHWERTMANN, U., 1982, Goethite and hematite in a climosequence in southern Brazil and their application in classification of kaolinitic soils: *Geoderma*, v. 29, p. 27–39.
- KRAUS, M.J., 1987, Integration of channel and floodplain suites, II. Lateral relations of alluvial paleosols: *Journal of Sedimentary Petrology*, v. 57, p. 602–612.
- KRAUS, M.J., 1996, Avulsion deposits in lower Eocene alluvial rocks, Bighorn Basin, Wyoming: *Journal of Sedimentary Research*, v. 66, p. 354–363.
- KRAUS, M.J., AND ASLAN, A., 1993, Eocene hydromorphic paleosols: significance for interpreting ancient floodplain processes: *Journal of Sedimentary Petrology*, v. 63, p. 453–463.
- KRAUS, M.J., AND ASLAN, A., 1999, Paleosol sequences in floodplain environments: a hierarchical approach, in Thiry, M. and Coincon, R.S., eds., *Palaeoweathering, Palaeosurfaces and Related Continental Deposits*: International Association of Sedimentologists, Special Publication 27, p. 303–321.
- KRAUS, M.J., AND BOWN, T.M., 1986, Paleosols and time resolution in alluvial stratigraphy, in Wright, V.P., ed., *Paleosols: Their Recognition and Interpretation*: Oxford, U.K., Blackwell Scientific, p. 180–207.
- LEEDER, M.R., 1978, A quantitative stratigraphic model for alluvium, with special reference to channel deposit density and interconnectedness, in Miall, A.D., ed., *Fluvial Sedimentology*: Canadian Society of Petroleum Geologists, Memoir 5, p. 587–596.
- MACEDO, J., AND BRYANT, R.B., 1987, Morphology, mineralogy, and genesis of a hydrosequence of Oxisols in Brazil: *Soil Science Society of America, Journal*, v. 51, p. 690–698.
- MACEDO, J., AND BRYANT, R.B., 1989, Preferential microbial reduction of hematite over goethite in a Brazilian Oxisol: *Soil Science Society of America, Journal*, v. 53, 1114–1118.
- MCCARTHY, P.J., MARTINI, I.P., AND LECKIE, D.A., 1997, Pedosedimentary history and floodplain dynamics of the Lower Cretaceous upper Blairmore Group, southwestern Alberta, Canada: *Canadian Journal of Earth Sciences*, v. 34, p. 598–617.
- MOHRIG, D., HELLER, P.L., PAOLA, C., AND LYONS, W.J., 2000, Interpreting avulsion process from ancient alluvial sequences: Guadalupe–Matarranya system (northern Spain) and Wasatch Formation (western Colorado): *Geological Society of America, Bulletin*, v. 112, p. 1787–1803.
- MORA, C.I., AND DRIESE, S.G., 1999, Palaeoenvironment, palaeoclimate and stable carbon isotopes of Palaeozoic red-bed palaeosols, Appalachian Basin, U.S.A. and Canada, in Thiry, M., and Coincon, R.S., eds., *Palaeoweathering, Palaeosurfaces and Related Continental Deposits*: International Association of Sedimentologists, Special Publication 27, p. 61–84.
- NEASHAM, J.W., AND VONDRA, C.F., 1972, Stratigraphy and petrology of the lower Eocene Willwood Formation, Bighorn Basin, Wyoming: *Geological Society of America, Bulletin*, v. 83, p. 2167–2180.
- PIPUJOL, M.D., AND BUURMAN, P., 1994, The distinction between ground-water gley and surface water gley phenomena in Tertiary paleosols of the Ebro basin, NE Spain: *Palaeogeography, Palaeoclimatology, Palaeoecology*, v. 110, p. 103–113.
- PIPUJOL, M.D., AND BUURMAN, P., 1997, Dynamics of iron and calcium carbonate redistribution and palaeohydrology in middle Eocene alluvial paleosols of the southeast Ebro Basin margin (Catalonia, northeast Spain): *Palaeogeography, Palaeoclimatology, Palaeoecology*, v. 134, p. 87–107.
- PLATT, N.H., AND KELLER, B., 1992, Distal alluvial deposits in a foreland basin setting—the Lower freshwater Molasse (lower Miocene), Switzerland: *sedimentology, architecture and palaeosols*: *Sedimentology*, v. 39, p. 545–565.
- RETALLACK, G.J., 1990, *Soils of the Past*: Boston, Unwin Hyman, 520 p.
- SCHWERTMANN, U., 1993, Relations between iron oxides, soil color, and soil formation, in Bigham, J.M., and Ciolek, E.J., eds., *Soil Color*: Soil Science Society of America, Special Publication 31, p. 51–69.
- SOIL SURVEY STAFF, 1975, *Soil Taxonomy*: Washington, D.C., U.S. Department of Agriculture, Handbook 436, 754 p.
- SOIL SURVEY STAFF, 1998, *Keys to Soil Taxonomy* [microform], 8th Edition, Washington, D.C., U.S. Department of Agriculture, Natural Resources Conservation Service, 326 p.
- SPRECHER, S.W., 2001, Basic concepts of soil science, in Richardson, J.L., and Vepraskas, M.J., eds., *Wetland Soils*: Boca Raton, Florida, Lewis Publishers, p. 3–18.
- STOLT, M.H., OGG, C.M., AND BAKER, J.C., 1994, Strongly contrasting redoximorphic patterns in Virginia Valley and Ridge paleosols: *Soil Science Society of America, Journal*, v. 58, p. 477–484.
- VEPRASKAS, M.J., 1994, *Redoximorphic Features for Identifying Aquic Conditions*: North Carolina Agricultural Research Service, Technical Bulletin 301, 33 p.
- VEPRASKAS, M.J., WILDING, L.P., AND DREES, L.R., 1992, Aquic conditions for soil taxonomy: concepts, soil morphology and micromorphology, in Ringrose-Voase, A.J., and Humphreys, G.S., eds., *Soil Micromorphology: Studies in Management and Genesis*: Amsterdam, Elsevier, *Developments in Soil Science* 22, p. 117–131.
- WAMBEKE, A.V., 1992, *Soils of the Tropics: Properties and Appraisal*: New York, McGraw-Hill, Inc., 343 p.
- WEISSMANN, G.S., 1988, Alluvial architecture of a sheet sandstone, Willwood Formation, Bighorn Basin, Wyoming [unpublished M.S. thesis]: University of Colorado, Boulder.
- WILDING, L.P., AND TESSIER, D., 1988, Genesis of Vertisols: shrink–swell phenomena, in Wilding, L.P., and Puentes, R., eds., *Vertisols: Their Distribution, Properties, Classification, and Management*: College Station, Texas A&M, Technical Monograph 18, p. 205–225.
- WING, S.L., 1981, A study of paleoecology and paleobotany in the Willwood Formation (early Eocene, Wyoming) [unpublished Ph.D. thesis]: Yale University, New Haven, 391 p.
- WING, S.L., BAO, H., AND KOCH, P.L., 1999, An early Eocene cool period? Evidence for continental cooling during the warmest part of the Cenozoic, in Huber, B.T., Macleod, K.G., and Wing, S.L., eds., *Warm Climates in Earth History*: Cambridge, U.K., Cambridge University Press, p. 197–237.
- WRIGHT, V.P., 1992, Paleopedology: stratigraphic relationships and empirical models, in Martini, I.P., and Chesworth, W., eds., *Weathering, Soils and Paleosols*: Amsterdam, Elsevier, p. 475–499.
- WRIGHT, V.P., TAYLOR, K.G., AND BECK, V.H., 2000, The paleohydrology of Lower Cretaceous seasonal wetlands, Isle of Wight, Southern England: *Journal of Sedimentary Research*, v. 70, p. 619–632.
- YAALON, D.H., AND KALMAR, D., 1978, Dynamics of cracking and swelling clay soils: displacement of skeletal grains, optimum depth of slickensides, and rate of intra-pedonic turbation: *Earth Surface Processes*, v. 3, p. 31–42.
- ZALEHA, M.J., 1997, Siwalik paleosols (Miocene, northern Pakistan): genesis and controls on their formation: *Journal of Sedimentary Research*, v. 67, p. 821–839.

Received 22 June 2001; accepted 17 December 2001.